IJC
International Journal of Cancer

Selective depletion of tumor neovasculature by microbubble destruction with appropriate ultrasound pressure

Junfen Wang[1]*, Zonglei Zhao[1,2]*, Shuxin Shen[1,2], Chuanxi Zhang[1], Shengcun Guo[1], Yongkang Lu[1], Yanmei Chen[1], Wangjun Liao[3], Yulin Liao[1]ô, and Jianping Bin[1]

[1] State Key Laboratory of Organ Failure Research, Department of Cardiology, Nanfang Hospital, Southern Medical University, Guangzhou, China
[2] Department of Cardiology, Henan Provincial People's Hospital, Zhengzhou University, Zhengzhou, China
[3] Department of Oncology, Nanfang Hospital, Southern Medical University, Guangzhou, China

Low-intensity ultrasound-microbubble (LIUS-MB) treatment is a promising antivascular therapy for tumors. We sought to determine whether LIUS-MB treatment with an appropriate ultrasound pressure could achieve substantial and persistent cessation of tumor perfusion without having significant effects on normal tissue. Further, we investigated the mechanisms underlying this treatment. Murine S-180 sarcomas, thigh muscles, and skin tissue from 60 tumor-bearing mice were subjected to sham therapy, an ultrasound application combined with microbubbles in four different ultrasound pressures (0.5, 1.5, 3.0, 5.0 MPa), or ultrasound at 5.0 MPa alone. Subsequently, contrast-enhanced ultrasonic imaging and histological studies were performed. Tumor microvessels, tumor cell necrosis, apoptosis, tumor growth, and survival were evaluated in 85 mice after treatment with the selected ultrasound pressure. We found that twenty-four hours after LIUS-MB treatment at 3.0 MPa, blood perfusion and microvessel density of the tumor had substantially decreased by 84 ± 8% and 84%, respectively ($p < 0.01$). Similar reductions were not observed in the muscle or skin. Additionally, an extreme reduction in the number of immature vessels was observed in the tumor (reduced by 90%, $p < 0.01$), while the decrease in mature vessels was not significant. Further, LIUS-MB treatment at 3.0 MPa promoted tumor cell necrosis and apoptosis, delayed tumor growth, and increased the survival rate of tumor-bearing mice ($p < 0.01$). These findings indicate that LIUS-MB treatment with an appropriate ultrasound pressure could selectively and persistently reduce tumor perfusion by depleting the neovasculature. Therefore, LIUS-MB treatment offers great promise for clinical applications in antivascular therapy for solid tumors.

Antivascular therapy is an important treatment modality for solid tumors.[1–3] However, antiangiogenic agents have shown limited success in clinical practice because of drug resistance[4,5] and systemic adverse effects.[6,7] Low-intensity ultrasound-microbubble (LIUS-MB) treatment, which combines of LIUS exposure and microbubbles, is a promising alternative method of targeting the tumor neovasculature. In this approach, the ultrasound-driven cavitation of microbubbles causes direct and localized mechanical damage to the vessel walls,[8] thereby decreasing tumor perfusion.[9,10] Furthermore, a series of previous studies have demonstrated that tumor vessels are more sensitive to LIUS-MB treatment than are the vessels in contiguous normal tissues.[10–12]

Key words: low-intensity ultrasound, microbubbles, antivascular therapy, tumor neovasculature

Abbreviations: ANOVA: analysis of variance; CEU: contrast-enhanced ultrasound; DMEM: Dulbecco's modified Eagle's medium; FBS: fetal bovine serum; H&E: hematoxylin and eosin; LIUS-MB: low-intensity ultrasound-microbubble; MVD: microvessel density; RBCs: red blood cells; SMA: smooth muscle actin; TUNEL: terminal deoxynucleotidyltransferase-mediated dUTP nick-end labelling; US: ultrasound; US-MB: ultrasound-microbubble; VI: video intensity

Additional Supporting Information may be found in the online version of this article.

Conflict of Interest Disclosures: All authors have declared that no conflicts of interest exist in regard to this work.

*J.W. and Z.Z. contributed equally to this work.

Grant sponsor: National Basic Research Program of China (973 Program); **Grant number:** 2013CB733804; **Grant sponsor:** National Natural Science Foundation of China; **Grant numbers:** 81227801 and 81271640; **Grant sponsor:** Natural Science Foundation of Guangdong Province (Team Program), China; **Grant number:** S2011030003134

DOI: 10.1002/ijc.29597

History: Received 4 Dec 2014; Accepted 30 Apr 2015; Online 7 May 2015

Correspondence to: Jianping Bin, MD, PhD, Department of Cardiology, Nanfang Hospital, Southern Medical University, 1838 N Guangzhou Ave, Guangzhou 510515, China, Tel.: (+86) 20-61642365, Fax: (+86) 20-87712332, E-mail: jianpingbin@126.com or jianpingbin@hotmail.com

What's new?
Selectively disrupting the flow of blood to solid tumors can halt tumor growth. But doing so clinically with antiangiogenic drugs is complicated by side effects, and the benefits often are transitory, owing to tumor cell resistance. An alternative to antiangiogenic drugs may be low-intensity ultrasound-microbubble (LIUS-MB) treatment. Here, in mice, LIUS-MB treatment delivered at 3.0 MPa resulted in immediate cessation of tumor perfusion, with effects lasting 24 hours. The same treatment had only minor effects on perfusion in normal tissue. Though the mechanism remains unclear, at 3.0 MPa LIUS-MB treatment selectively depletes the tumor vasculature of immature, defective microvessels.

It is believed that the use of appropriate ultrasound parameters could achieve a nearly complete and persistent cessation of tumor blood flow without normal tissue injury, which is the essential basis for the clinical application of LIUS-MB treatment. However, there is a lack of experimental data that validates this assumption, which has mainly been attributed to the limitations of previous studies' research designs. Most of these were focused on the antitumor efficacy of LIUS-MB treatment and either overlooked its adverse effects on normal tissues[9,13] or investigated the immediate effect on tumor perfusion without follow-up observations.[9,11,12] Only one study has evaluated the short- and long-term effects of LIUS-MB treatment on blood perfusion in both the tumor and surrounding tissues.[10] However, the study failed to determine the appropriate ultrasound condition and, therefore, its findings were too weak to validate the hypothesized potential of LIUS-MB treatment.

Evidence is also lacking in regard to the histological basis of tumor vessels' increased susceptibility to LIUS-MB treatment, as compared with normal vessels. The greater susceptibility of tumor vessels might be ascribed to the defective structures of the tumor neovasculature, but the underlying explanation remains to be clarified. Furthermore, although the accumulated evidence has shown that LIUS-MB treatment's ability to immediately decrease tumor perfusion is attributable to vascular dilation,[11,13,14] thrombosis,[9,12] and disruption,[10,15] the mechanism that is responsible for the persistent cessation of tumor blood flow remains poorly understood. There is an abundance of evidence to suggest that tumors' sustained perfusion deficiency during antivascular therapy is always associated with a significant reduction in microvessel density (MVD),[16,17] indicating that the substantial killing of endothelial cells and the resultant vascular depletion may play an important role in the permanent shutdown of tumor blood flow that results from LIUS-MB treatment.

It is recognized that acoustic cavitation, especially inertial cavitation, plays a critical role in the antivascular effects elicited by LIUS-MB treatment.[10,18,19] It is also recognized that ultrasound pressure is one of the most important parameters for the inertial cavitation.[20,21] In the light of these previous findings, we hypothesized that the use of LIUS-MB treatment with appropriate ultrasound pressure could result in substantial and persistent damage to tumor perfusion, while having minor effects on normal tissues. Further, we hypothesized that LIUS-MB treatment with the appropriate pressure mainly achieves the selective and persistent reduction of tumor perfusion through the depletion of tumor neovasculature that features defective construction, resulting in long-term tumor remission and improved survival.

Material and Methods

The study was approved by the Animal Research Committee of the Southern Medical University and was performed in accordance with the NIH Guide for the Care and Use of Laboratory Animals.

Tumor model and experimental protocol

Mouse sarcoma S-180 cells were obtained from the cell bank of Sun Yat-sen University (Guangzhou, China). Cells were cultured in Dulbecco's modified Eagle's medium (DMEM, Invitrogen, Carlsbad, CA) with 10% fetal bovine serum (FBS; Invitrogen). Cells (2×10^6 cells) were then injected subcutaneously in the left hind limbs of male Kunming mice (6–8 weeks old and weighing 23–30 g, purchased from the Laboratory Animal Centre of Southern Medical University). LIUS-MB treatment was performed 7 days after tumor implantation, when the tumor reached a size of approximately 10 mm in diameter.

To determinate an appropriate level of ultrasound pressure, 60 tumor-bearing mice were randomly divided into a sham group and five treatment groups ($n = 10$ per group) for experimentation on the tumors in their left hind limbs. The thigh muscles and skin of their right hind limbs were used to provide normal controls. The left or right hind limb was covered with a foam pad while the collateral limb was insonated. The sham treatment was performed with the therapeutic ultrasound transducer in the off setting. The five treatment groups were divided into four ultrasound-microbubble treatment (US-MB treatment) groups and an ultrasound treatment (US treatment) group. The US-MB treatment groups were insonated with differentiated peak negative acoustic pressures (0.5, 1.5, 3.0, and 5.0 MPa) in the presence of microbubbles, while the US treatment group was insonated with 5.0-MPa ultrasound in the absence of microbubbles. For five of the ten mice per group, serial B-mode and contrast-enhanced ultrasonic (CEU) perfusion imaging of the tumor and muscles were performed on three occasions: before treatment, immediately after treatment (0 hr), and 24 hr after treatment. These animals were sacrificed at 24 hr, whereas the other five mice in each group were sacrificed immediately after treatment (0 hr). Tumors, thigh muscles, and skin tissue

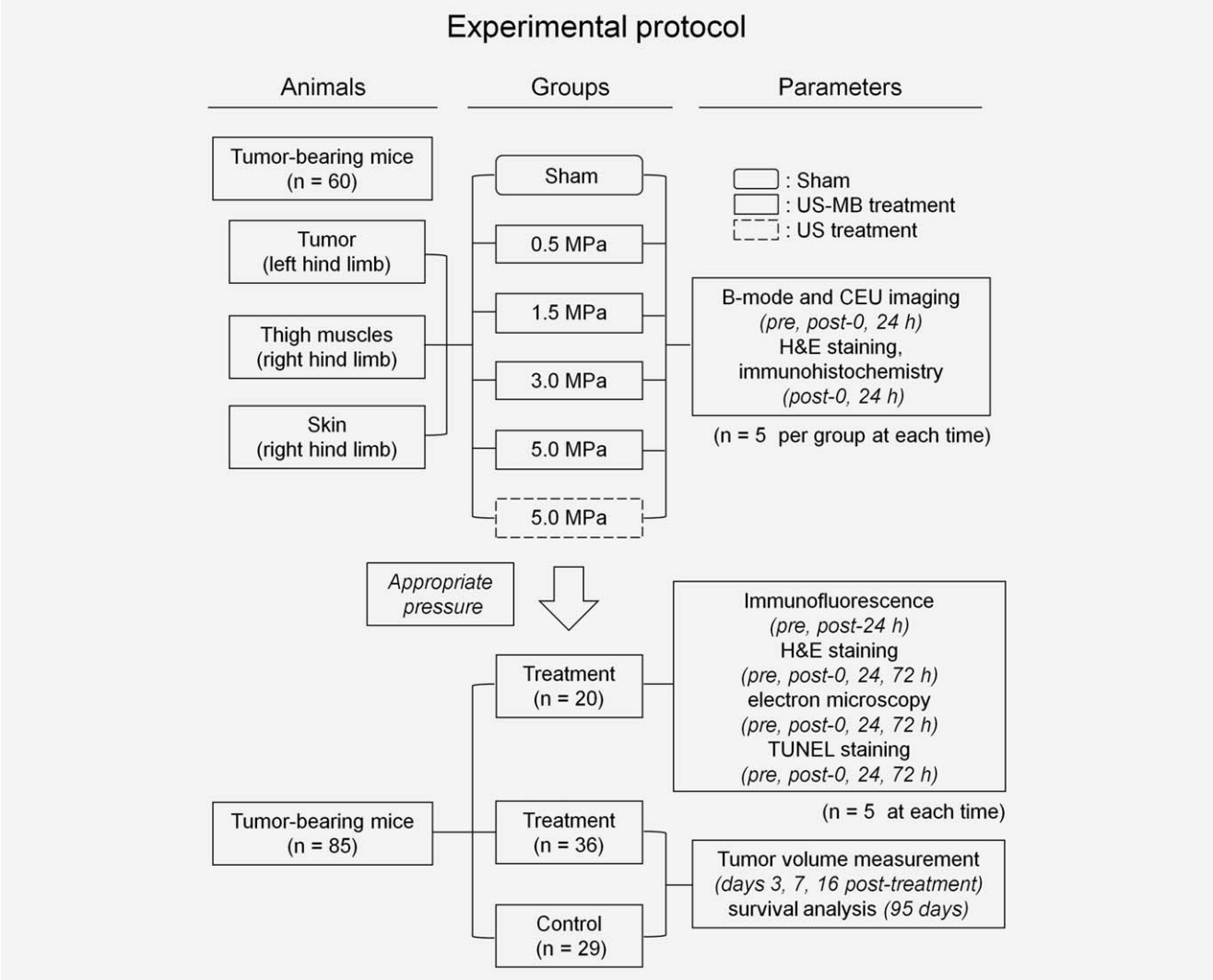

Figure 1. Illustration of the experimental protocol. CEU, contrast-enhanced ultrasound; H&E, hematoxylin and eosin. See text for details.

were then collected for hematoxylin and eosin (H&E) and immunohistochemical staining. Mice were sacrificed using an overdose of anesthesia (pentobarbital sodium 150 mg/kg, ip) and cervical dislocation.

To explore the mechanism by which tumor vessels are more susceptible to LIUS-MB treatment than are normal vessels, we applied the immunofluorescent double-labeling method to the tumors and muscles both before and 24 hr after LIUS-MB treatment, which was performed using the appropriate ultrasound pressure that had been determined earlier ($n = 5$ on each occasion).

To evaluate the therapeutic effect of LIUS-MB treatment at the appropriate pressure level, H&E staining, transmission electron microscopy, and TUNEL (terminal deoxynucleotidyl-transferase-mediated dUTP nick-end labeling) staining were performed before treatment, as well as 0, 24, and 72 hr after treatment ($n = 5$ on each occasion). Meanwhile, 65 tumor-bearing mice were randomly divided into a treatment group ($n = 36$) and a control group ($n = 29$); the treatment group was insonated on day 7 after tumor implantation, while the control group did not undergo insonation. Tumor volume was measured with B-mode ultrasound imaging on days 0, 3, 7, and 16 post-treatment. Animals were followed for up to 95 days after the tumor implantation to determine their survival outcomes. The experimental protocol is also illustrated in Figure 1.

Supplementary *in vivo* experiments were carried out to assess the tissue temperature during the treatment (see Supporting Information for details).

B-mode and CEU perfusion imaging

B-mode and CEU perfusion imaging of the tumor and thigh muscles were performed using an ultrasound system with a 15L8 transducer (Sequoia512; Siemens Medical Systems, Mountain View, CA). Lipid-shelled perfluoropropane microbubbles were prepared by the high speed shearing method

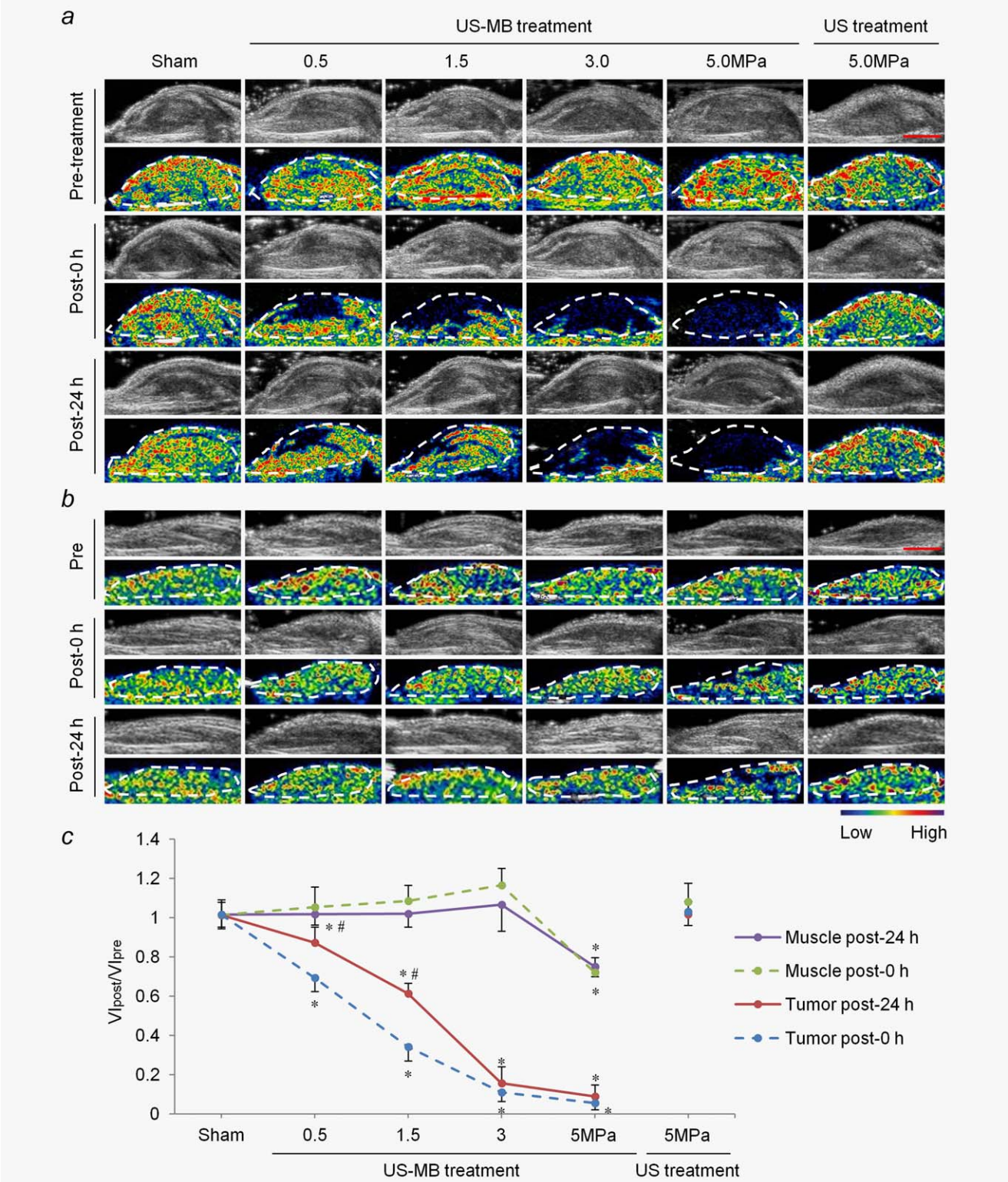

Figure 2. Effects of LIUS-MB treatment on blood perfusion in the tumor and muscle over time: results for various pressures. Representative B-mode and background-subtracted color-coded images of the tumor (*a*) and muscle (*b*) from one animal in each group. (*c*) Quantitative analysis of the change in blood perfusion. $^{*}p < 0.01$ *vs*. the respective sham groups. $^{\#}p < 0.05$ *vs*. the $VI_{post\text{-}0\ hr}/VI_{pre}$. VI, video intensity. Scale bar = 0.5 cm. [Color figure can be viewed in the online issue, which is available at wileyonlinelibrary.com.]

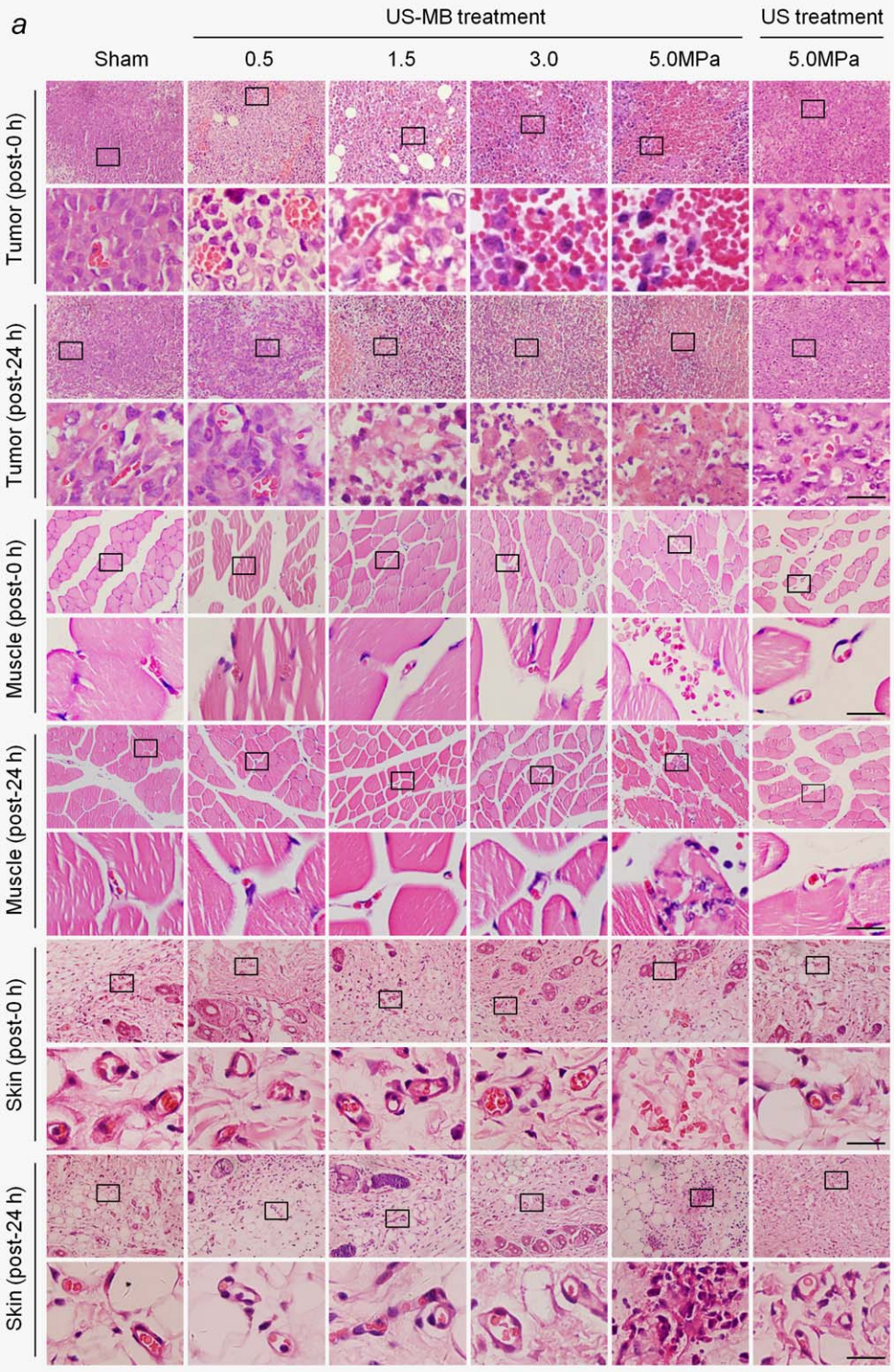

Figure 3. Effects of LIUS-MB treatment on microvessels in the tumor, muscle, and skin, as well as their relationships with corresponding blood perfusion: results for various pressures. Hematoxylin-eosin (*a*) and immunohistochemical staining for the endothelial marker CD31 (*b*) in the tumor, muscle, and skin. (*c*) Quantitative analysis of the MVD at 24 hr after treatment. Correlations between VI data obtained by CEU imaging and the MVD at 24 hr after treatment in the tumor (*d*) and muscle (*e*). $^{\#}p < 0.05$, $^{*}p < 0.01$ *vs*. the respective sham groups. MVD, microvessel density; HPF, high power field; VI, video intensity; CEU, contrast-enhanced ultrasound. Scale bar = 20 μm. [Color figure can be viewed in the online issue, which is available at wileyonlinelibrary.com.]

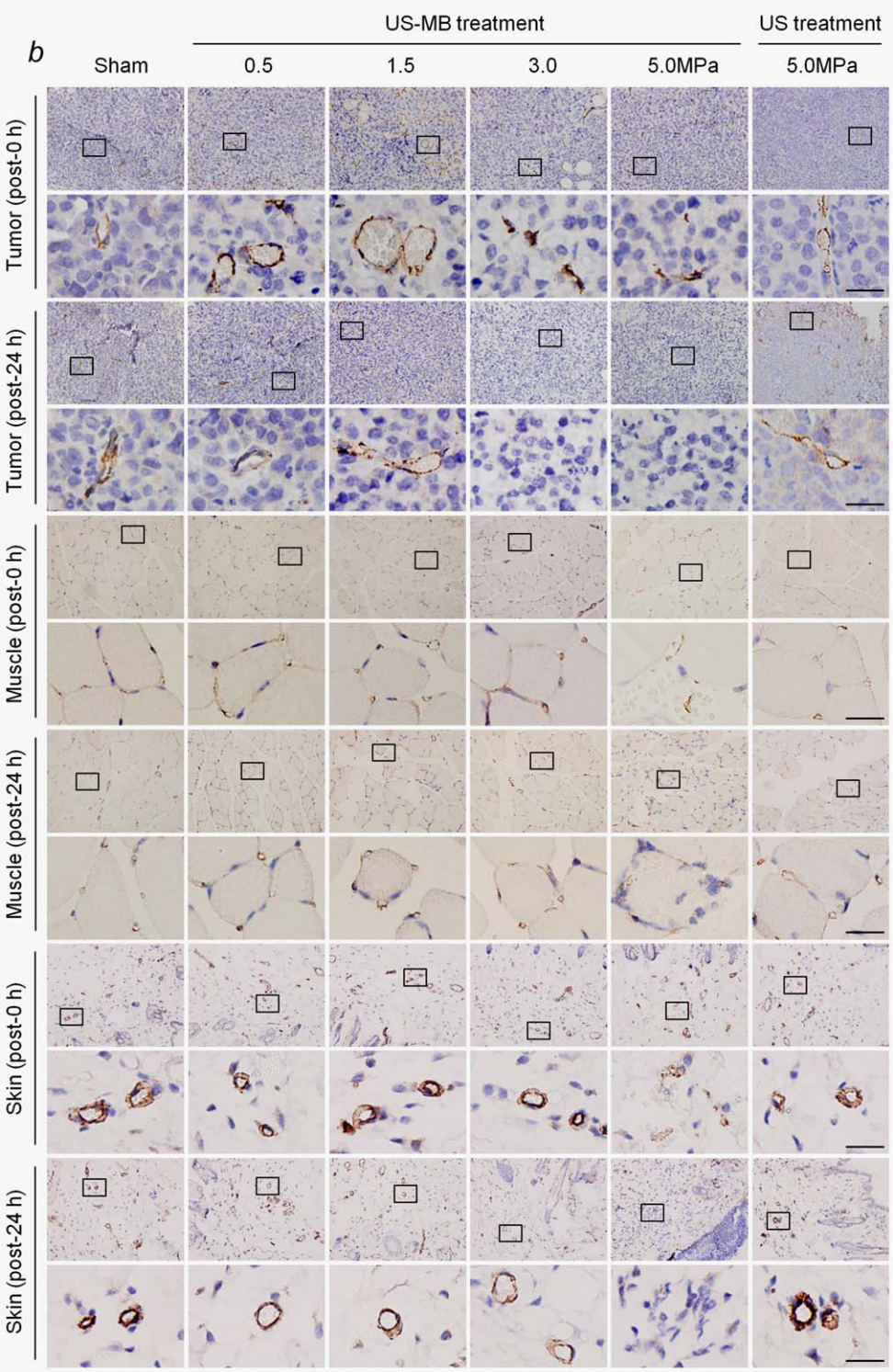

Figure 3. Continued

(see Supporting Information for details). Mice were anesthetized and placed in ventral recumbency. An initial B-mode imaging was performed at a mechanic index of 0.27. After intravenous injection of a bolus of 3×10^7 microbubbles, CEU perfusion imaging was performed with contrast pulse sequencing at a centerline frequency of 7 MHz and a mechanic index of 0.17. To determine the signal from the circulating microbubbles alone, post-contrast frames were digitally subtracted by a precontrast frame using software (Yabko MCE2.7; University of Virginia, Charlottesville, VA)

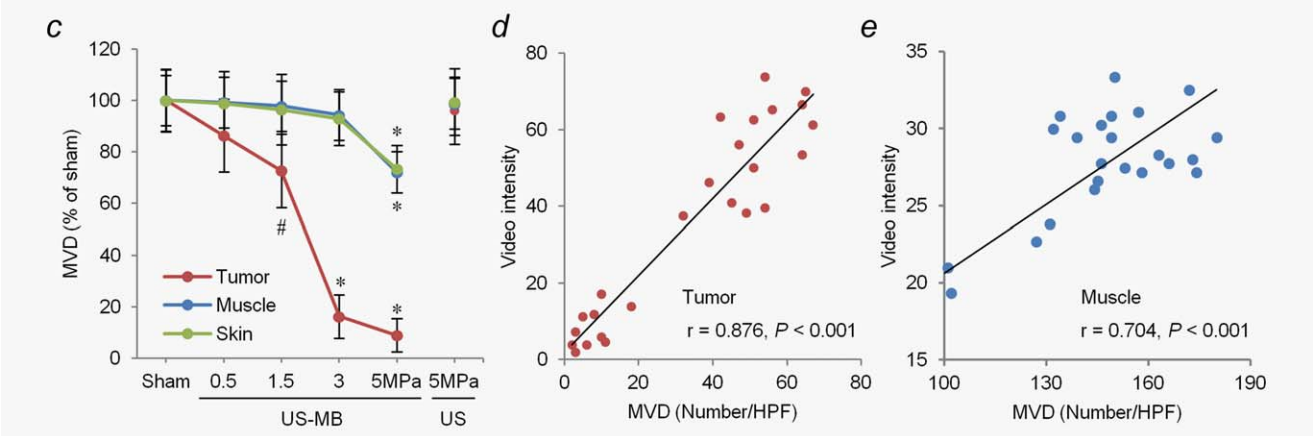

Figure 3. Continued

and then color coded. To eliminate the influence of ultrasound attenuation in the femur, background-subtracted signals were measured from a region of interest located between the transducer and the femur. A time-intensity curve of contrast signals was then plotted and the peak intensity value was employed for comparisons.

Tumor volume was assessed using B-mode ultrasound imaging at a mechanic index of 0.27. In each of the B-mode images, the length (L) and width (W) of the tumor were measured. Tumor volume (V) was then calculated as follows: $\pi \times (L \times W^2)/6$.[22]

Low-intensity ultrasound treatment

LIUS treatment was performed using a pulsed therapeutic ultrasound device with a KHT-017 transducer (DCT-700, Shenzhen Well.D Medical Electronic, Shenzhen, China). To maintain a distance of 5 mm between the transducer and the skin overlying the tumor or thigh muscles, the transducer was fixed on a steel stand with scale. Subsequently, ultrasound coupling gel was applied to the skin. Treatment was initiated at least 15 min after the disappearance of all contrast agent from the previous CEU perfusion imaging. The US-MB treatment was applied to the tumor or the thigh muscles and skins after intravenous injection of a bolus of 1.5×10^8 microbubbles, while the US treatment was performed in the absence of microbubbles. The transducer was operated at a frequency of 0.94 MHz with a pulse repetition frequency of 10 Hz and a duty cycle of 0.19%. The treatment was performed using an intermittent mode of 3 sec on and 9 sec off for 1 min.

Histological examinations and apoptosis assay

After the mice were sacrificed, the tumors, thigh muscles, and skins were rapidly excised and cut into several pieces for the different histological studies. Specimens were fixed with 4% paraformaldehyde and paraffin-embedded for H&E, immunohistochemical, and TUNEL staining.

To measure the necrotic area in the tumor, 4–6 μm sections were stained with H&E. The area of necrosis was identified and quantified independently by two experienced investigators using an optical microscope (OLYMPUS BX51, Olympus Optical, Tokyo, Japan).

To evaluate the MVD, sections were incubated with anti-PECAM-1 (anti-mouse CD31 antibody, Santa Cruz Biotechnology, Santa Cruz, CA) to stain for endothelial cells. Density counts of microvessels were also performed independently by two investigators, as described previously.[23,24]

To determine the apoptosis level, TUNEL assay was performed using a TMR red kit (Roche, Shanghai, China) as previously described.[25] The rate of TUNEL-labeled cells was calculated from three randomly selected areas under an epifluorescence microscope (OLYMPUS BX51, Olympus Optical, Tokyo, Japan).

Confocal immunofluorescence and transmission electron microscopy

Tumors and thigh muscles were cryopreserved and embedded in optimal cutting temperature compound (Tissue-Tek, SAKURA Finetek USA, Torrance, CA) for immunofluorescence staining. Five-μm sections were incubated with anti-CD31 (Abcam, Cambridge, UK) and anti-α-smooth muscle actin (SMA; Abcam) antibodies to detect endotheliocytes and pericytes, respectively. Nuclei were stained with DAPI (Sigma-Aldrich, St. Louis, MO). A pericyte-positive microvessel was defined as a CD31-positive microvessel surrounded by at least one cell staining positive for α-SMA.

For the ultrastructural observations, specimens were prepared as described elsewhere[26] and slides were visualized under a transmission electron microscope (JEM-2010HR, JEOL, Tokyo, Japan).

Statistical analysis

Multiple comparisons were performed using one-way analysis of variance (ANOVA) followed by a Bonferroni correction. The least-squares method was employed to assess linear correlations between selected variables. Comparisons of tumor volume between two groups were performed using repeated-measures ANOVA. Kaplan–Meier curves and log-rank tests

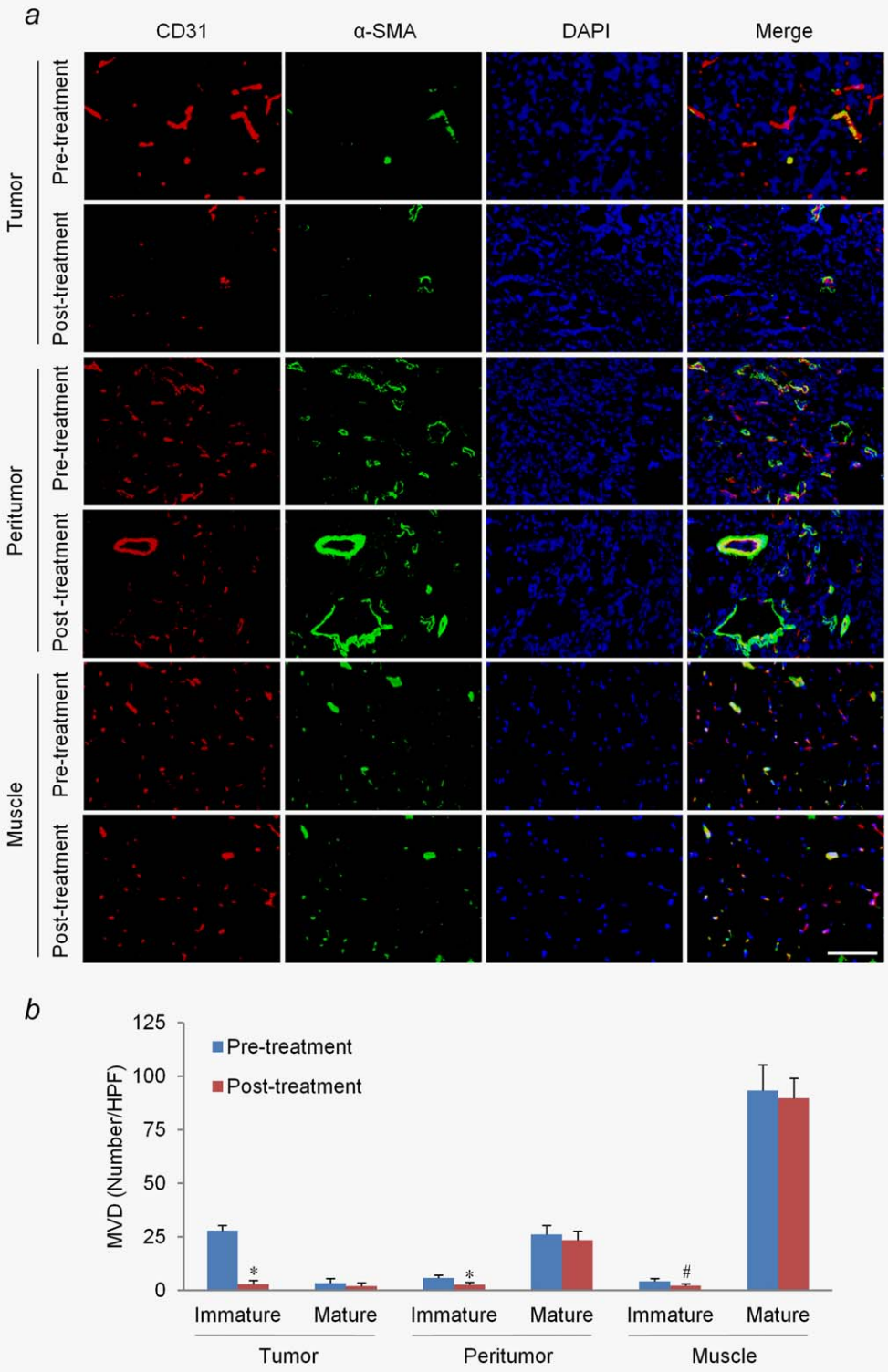

Figure 4. Effects of LIUS-MB treatment with 3.0 MPa on vessels of different maturity. (*a*) Confocal immunofluorescence of vessels in the tumor, peritumor tissue, and muscle for CD31 (red) and α-SMA (green). (*b*) Quantitative analysis of immature and mature microvessels. $^{\#}p < 0.05$, $^{*}p < 0.01$ *vs*. their corresponding baselines (pretreatment). SMA, smooth muscle actin. Scale bar = 100 μm. [Color figure can be viewed in the online issue, which is available at wileyonlinelibrary.com.]

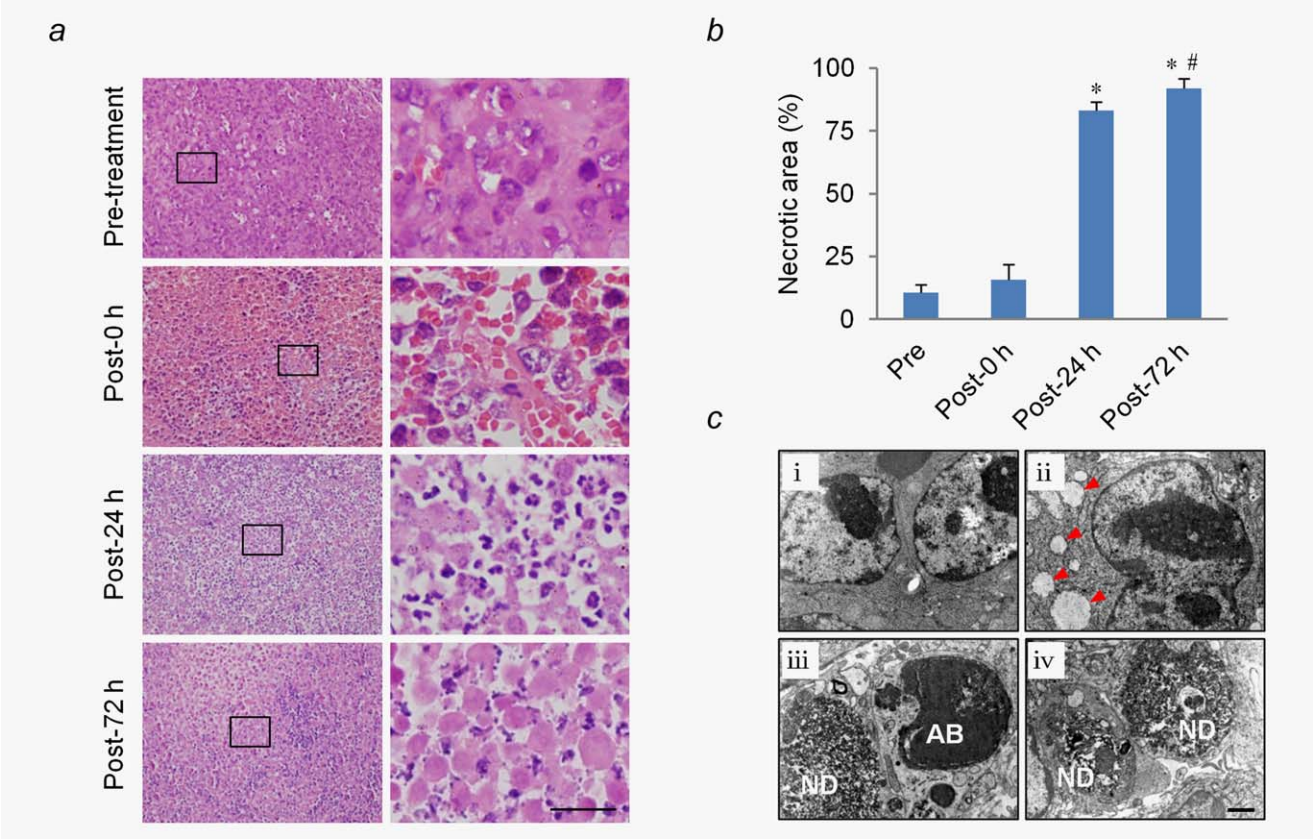

Figure 5. LIUS-MB treatment promotes cell necrosis and apoptosis in tumor, but not in muscle or skin. Hematoxylin-eosin staining (*a*) and quantification of the necrosis area (*b*) in the tumor. Scale bar = 20 μm. (*c*) Representative transmission electronic micrographs of tumor cells before treatment (i), as well as 0 (ii), 24 (iii), and 72 hr (iv) after treatment. Ultrastructural pathological changes were observed after treatment, including mitochondria swelling, vacuolation (ii; arrows), nuclear debris (iii, iv; ND) and apoptotic bodies (iii; AB). Scale bar = 0.5 μm. TUNEL staining and quantification of the apoptotic cells in the tumor (*d*), muscle (*e*), and skin (*f*). Scale bar = 50 μm. $^{*}p < 0.01$ *vs*. pre-treatment. $^{\#}p < 0.05$, $^{\&}p < 0.01$, *vs*. post-24 hr. [Color figure can be viewed in the online issue, which is available at wileyonlinelibrary.com.]

were used to estimate and compare the survival of different groups. Data were expressed as mean ± standard deviation and $p < 0.05$ was considered to indicate statistical significance. Statistical analyses were performed using SPSS 16.0 (IBM SPSS, Chicago, IL).

Results

The effects of LIUS-MB treatment on tumor, muscle, and skin: Results for various pressures

In the US-MB treatment groups with 3.0 and 5.0 MPa, tumor perfusion was substantially reduced immediately after treatment ($p < 0.01$) without significant recovery for 24 hr. In the US-MB treatment groups with 0.5 and 1.5 MPa, tumor perfusion was partially reduced immediately after treatment ($p < 0.01$) and gradually recovered thereafter ($p < 0.05$; Figs. 2a and 2c). In contrast to the tumor results, there was no significant reduction of blood perfusion in the muscle after US-MB treatment using 0.5, 1.5, or 3.0 MPa. However, blood perfusion in the muscle decreased by 28 ± 8% immediately after US-MB treatment with 5.0 MPa ($p < 0.01$) without significant recovery for 24 hr (Figs. 2b and 2c). In the 5.0-MPa US treatment group, neither tumor nor muscle perfusions showed significant changes after treatment (Figs. 2a–2*c*).

H&E staining showed that immediately after treatment, tumor microvessels were severely disrupted with their tubular architectures invisible and diffuse hemorrhage in the 3.0- and 5.0-MPa US-MB treatment groups. The degree of microvessel injury was milder in the 0.5- and 1.5-MPa US-MB treatment groups, as evidenced by vasodilation, congestion and hemorrhage. Greater acoustic pressures were accompanied by more extensive extravasation of red blood cells (RBCs) into the interstitial space of the tumor. At 24 hr after treatment, the number of extravasated RBCs was reduced in all the US-MB treatment groups. Meanwhile, massive necrosis of tumor cells was observed in the US-MB treatment groups using 3.0 and 5.0 MPa, whereas the areas of necrosis were much smaller in the US-MB treatment groups using 0.5 and 1.5 MPa (Fig. 3a). In contrast with these tumor findings, there was no significant hemorrhage in the muscle or skin immediately after US-MB treatment using 0.5, 1.5, or 3.0 MPa. Consistently, we did not observe significant cell necrosis in the muscle or skin at 24 hr

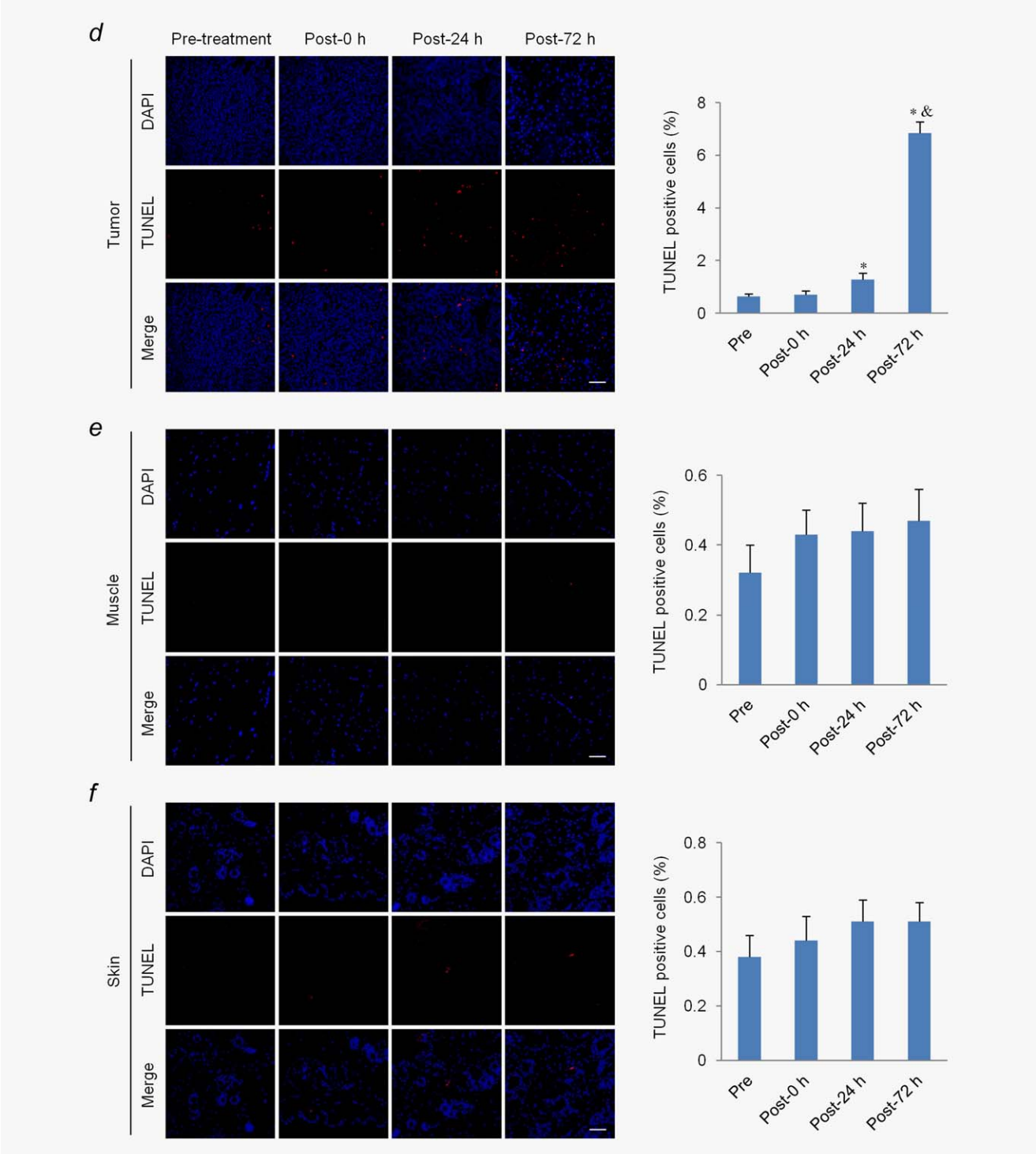

Figure 5. Continued

post-treatment. However, we noted microvessel rupture sites with a large quantity of RBCs in the interstitial space of the muscle and skin, immediately after US-MB treatment with 5.0 MPa. At 24 hr after treatment, inflammatory cell infiltrate and necrosis were observed in the muscle and skin. In the US treatment group with 5.0 MPa, extravasated RBCs and cell necrosis were not obviously noted in the tumor, muscle or skin, either immediately or at 24 hr after treatment (Fig. 3a).

The results of immunohistochemistry further revealed that immediately after US-MB treatment using 3.0 and 5.0 MPa, the structures of tumor microvessels were incomplete, with vessel fragments scattered in the region. In the US-MB treatment groups

with 0.5 and 1.5 MPa, the diameters of tumor microvessels appeared to increase, as compared with the sham group (Fig. 3b). In contrast, microvessels in the muscle and skin were mostly circular and clearly visible in the 0.5-, 1.5-, and 3.0-MPa groups, while a great number of ruptured microvessels were observed in the 5.0-MPa group immediately after US-MB treatment. In the 5.0-MPa US treatment group, no microvessel ruptures were seen in the tumor, muscle, or skin immediately after treatment (Fig. 3b).

Twenty-four hours after treatment, there was a significant reduction in the MVD of the tumor in the US-MB treatment groups with 1.5, 3.0, and 5.0 MPa, as compared with the sham group. The MVD of the tumor was reduced by 84 and 91% in the 3.0- and 5.0-MPa groups, respectively ($p < 0.01$), while it was reduced by 27% in the 1.5- MPa group ($p < 0.05$) of US-MB treatment (Figs. 3b and 3c). In contrast, there was no significant reduction in the MVD of the muscle or skin in the 0.5-, 1.5-, or 3.0-MPa groups, as compared with the sham group. However, the MVDs of the muscle and skin were decreased by 28 and 27% in the US-MB treatment group with 5.0 MPa, respectively ($p < 0.01$). In the 5.0-MPa US treatment group, there was no significant reduction in the MVD of the tumor, muscle, or skin (Figs. 3b and 3c). In addition, there were significant positive correlations between the video intensity (VI) data obtained from CEU imaging and the MVD at 24 hr post-treatment in the tumor and muscle ($p < 0.001$; Figs. 3d and 3e).

Selective depletion of tumor microvasculature based on blood vessel maturation

Next, we explored the mechanism for selective depletion of tumor microvasculature at the ultrasound pressure of 3.0 MPa, which was determined to be appropriate through the analysis described above. Confocal immunofluorescence staining showed that a majority of tumor microvessels lacked pericytes ($89 \pm 7\%$), which is denoted as an immature state. Unlike the tumor microvessels, only a small subset of microvessels in the peritumor tissue and muscle were immature ($19 \pm 5\%$ and $4 \pm 2\%$, respectively, Figs. 4a and 4b). Twenty-four hours after treatment, the number of immature microvessels was significantly reduced in these tissues, especially in the tumor tissues (reduced by 90%, $p < 0.01$), while there was no significant reduction in the number of mature vessels (Figs. 4a and 4b).

LIUS-MB treatment contributes to cell necrosis and apoptosis in tumor, but not in muscle or skin

We also investigated the effect of LIUS-MB treatment with 3.0 MPa on tumor cells. Tumor cells were grown in a solid pattern and only a few spots of cell necrosis were present before treatment. Immediately after treatment, there was no evidence of localized coagulative necrosis of tumor cells, while a large area of necrotic tissue was observed 24 hr after treatment, as indicated by a huge mass of karyorrhexis and karyolysis. The range of tumor necrosis further expanded and reached $92 \pm 4\%$ at 72 hr post-treatment (Figs. 5a and 5b).

Electronic microscopy results showed that the majority of tumor cells were large with clear nuclear membranes and rich euchromatin before treatment (Fig. 5c i). Immediately after treatment, mitochondrial swelling and vacuolation were noted in some of the tumor cells (Fig. 5c ii). Twenty-four hours after treatment, many necrotic tumor cells and a few apoptotic cells were observed, as evidenced by nuclear debris and apoptotic bodies, respectively (Fig. 5c iii). The number of necrotic tumor cells was further increased when evaluated 72 hr after treatment (Fig. 5c iv).

TUNEL assay results revealed that tumor cell apoptosis was significantly increased at 24 hr after treatment, as compared with the pretreatment ($p < 0.01$). Further, the amplitude of increase was even larger at 72 hr after treatment ($p < 0.01$; Fig. 5d). In contrast, there was no significant increase in the number of apoptotic cells in the muscle or skin after treatment (Figs. 5e and 5f).

LIUS-MB treatment reduces tumor growth rates and prolongs the survival of tumor-bearing mice

As shown in Figure 6a–6*c*, there was no significant difference in tumor volume between the treatment and control groups before treatment, whereas the tumor volume in the treatment group was significantly smaller than that in the control group at each measurement time after treatment (all $p < 0.01$). In addition, examination of the survival curves showed that the median survival time of mice in the treatment group was significantly longer than that in the control group (38 *vs*. 26 days, $p < 0.0001$, log-rank test; Fig. 6d).

Discussion

In this study, we found that LIUS-MB treatment with an appropriate ultrasound pressure of 3.0 MPa resulted in substantial and persistent damage to tumor perfusion, but had minor effects on normal tissue. The different effects of LIUS-MB treatment on tumor and normal tissue arose from the selective depletion of tumor neovasculature that featured defective construction. Consequently, delayed tumor growth and improved survival rates were obtained in a murine model after treatment with the appropriate ultrasound pressure.

It is generally believed that LIUS-MB treatment mainly exerts its antivascular effect through inertial cavitation; the violent collapse of intravenous microbubbles gives rise to transient microjets that produced mechanical force on the vessel wall,[27] leading to vessel injury or even rupture. Although LIUS-MB treatment with appropriate ultrasound parameters can theoretically confer excellent antitumor efficacy and minor side effects, the available data have been insufficient to fully validate this assumption and determine the appropriate ultrasound parameters. Ultrasound pressure is one of the most important parameters that determine the inertial cavitation.[20,21] In this study, we therefore designed and performed a series of comparative *in vivo* experimental observations, including assessments of blood perfusion, microvessel morphology, and microvessel quantity in tumor,

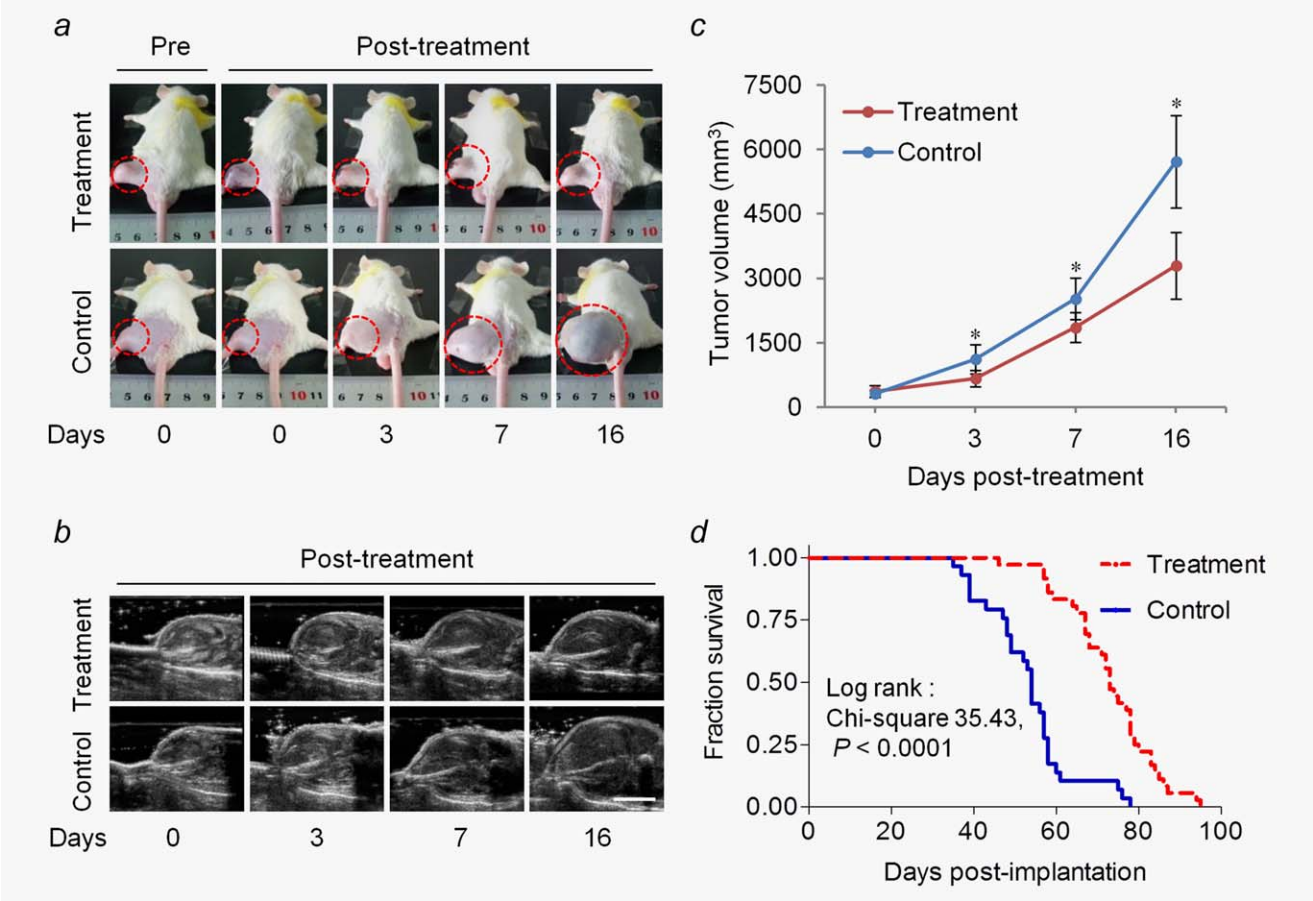

Figure 6. LIUS-MB treatment delays tumor growth and improves mouse survival. Representative pictures (*a*) and B-mode ultrasound images (*b*) of the tumor from one animal in each group. (*c*) Quantitative analysis of the tumor volume from B-mode images. (*d*) Kaplan–Meier survival curves for tumor-bearing mice with and without treatment. $*p < 0.01$ *vs*. the control group. Scale bar = 1 cm. [Color figure can be viewed in the online issue, which is available at wileyonlinelibrary.com.]

muscle, and skin. These assessments were conducted 0 and 24 hr after sham therapy, US-MB treatment with four different levels of ultrasound pressure, or US treatment at 5.0-MPa level, all of which were performed at a frequency of 0.94 MHz. After the US-MB treatment at 3.0 MPa, we found that tumor perfusion was markedly and persistently decreased, while there was no significant reduction in the perfusion of muscle. The histological observations consistently revealed that the tumor vessels were seriously disrupted and depleted, while the vessels in the muscle and skin were hardly affected. At the other three pressures of US-MB treatment, we noted either an incomplete and recoverable reduction of the tumor blood flow or a significant reduction in the perfusion of muscle. Meanwhile, we did not find any significant change in the tumor perfusion when US treatment was performed in the absence of microbubbles. These findings indicated that LIUS-MB treatment could achieve substantial and persistent cessation of tumor blood flow without significant effects on normal tissue, offering great promise for clinical use as an antivascular therapy. Further, our findings indicated that an ultrasound pressure of 3.0 MPa at a frequency of 0.94 MHz was appropriate for the tumor treatment. This conclusion is partly supported by a previous study,[10] in which LIUS-MB treatment was applied to tumors using acoustic pressures of 2.6 and 4.8 MPa and a similar frequency to our own (0.831 MHz). It should be noted that the effects of appropriate ultrasound pressure on other normal tissues should be investigated in future studies.

As would be expected, we observed that LIUS-MB treatment with the appropriate ultrasound pressure of 3.0 MPa had positive long-term efficacy, as evidenced by tumor growth delays and an improved survival rate, which is consistent with a few previous studies.[9,28] However, it was also reported that LIUS-MB treatment failed to inhibit the growth of medium-stage tumors in a tumor-bearing murine model.[29] These different therapeutic effects may be partially explained by the differences in the ultrasound energies that were applied. Indeed, more experiments are necessary to confirm the long-term efficacy of LIUS-MB treatment, especially with appropriate ultrasound parameters.

A series of previous studies have demonstrated that tumor vessels are more vulnerable to LIUS-MB treatment than are

the vessels of normal tissues.[10–12] It has been speculated that the defective structures of tumor neovessels may be responsible for this difference,[10,12] but this speculation had not been validated directly. Our immunofluorescence results showed that the large majority of tumor vessels were immature, while the vast majority of muscle vessels were mature, in accordance with previous studies.[30–32] The immature vessels are known to be structurally abnormal, and are characterized by widened endothelial gaps, defective basement membranes, and low rates of pericyte coverage.[30–32] After LIUS-MB treatment at the 3.0-MPa level, the immature vessels in the tumor and muscle were substantially depleted, while the mature vessels in both tissues resisted the effects of treatment and survived. These findings suggested that the defective construction of tumor neovessels should account for their increased vulnerability to LIUS-MB treatment. In addition, we noted that greater acoustic pressures were accompanied by greater reductions in the MVDs of the tumors, which is probably attributable to the structural heterogeneity of different subtypes of tumor vessels. However, this hypothesis needs to be proven in future studies, specifically by exploring the effects of LIUS-MB treatment on various tumor vessel subtypes. Until such studies are completed, we should remember that the appropriate ultrasound pressure may differ according to both the different mixtures of vessel subtypes in various tumors[33] and the heterogeneity of microvascular construction in different organs.[34]

This study has revealed that LIUS-MB treatment's ability to permanently shut down tumor blood flow is partially based on the severe damage to endothelial cells and the resultant depletion of tumor vessels. We found that tumor perfusion was substantially and persistently reduced immediately after treatment at the 3.0- and 5.0- MPa levels. H&E staining showed that the tumor vessels were severely disrupted under these conditions, with invisible vascular boundaries and a large quantity of RBCs extravasating into the interstitial space. Further, our immunohistological staining results consistently showed that the MVD of the tumor tissue was significantly reduced 24 hr post-treatment, indicating that the severe damage to tumor vessels had caused the death of endothelial cells and resultant vascular depletion. Moreover, we found a close correlation between the MVD and the lasting blood perfusion of the tumor, with perfusion decreasing in concordance with the decline in MVD. Accordingly, it is credible that the substantial depletion of tumor vasculature should at least in part contribute to the sustained and persistent cessation of tumor blood flow, which is essential to ensure antitumor efficacy.

In this study, we also found that there was no significant increase of tissue temperature during the treatment (Supporting Information Table S1). Consistently, immediately after treatment, there was no evidence of coagulation necrosis of tumor cells, which is usually associated with thermal ablation.[35,36] However, extensive tumor cell necrosis and apoptosis were noted 24 and 72 hr after treatment. These findings further support the previously suggested hypothesis that a sustained cessation of tumor blood flow, rather than direct damage to tumor cells, is responsible for the hindrance of tumor growth in LIUS-MB treatment. It should be mentioned that it is difficult to deplete tumor vessels completely using a single session of LIUS-MB treatment. Consequently, the residual tumor vessels would maintain a partial blood supply to the tumor and initiate a second phase of angiogenesis, accounting for the resurgence of tumor growth. Therefore, researchers should be encouraged to investigate whether multiple episodes of treatment can further reduce tumor burden and improve survival.

There are several limitations to our study. First, the bolus injection of contrast agent introduces challenges to the quantitative analysis of blood perfusion using CEU imaging. The peak intensity is known to be substantially correlated with the relative blood volume.[37] Accordingly, we employed this peak intensity as a representative of the blood perfusion, which is consistent with previous studies.[10,12,15] Second, this study only determined an appropriate ultrasound pressure level, and did not explore the therapeutic window of ultrasound pressure using comparative investigations with more intensive pressure gradients. Regarding the clinical feasibility of LIUS-MB treatment, it would be superior to determine a therapeutic window.

In conclusion, LIUS-MB treatment with an appropriate ultrasound pressure could selectively deplete tumor neovasculature that features defective construction, resulting in a substantial and permanent cessation of tumor blood flow without a significant effect on normal tissue, and consequently offering positive long-term efficacy.

ACKNOWLEDGMENTS

All authors have declared that no conflicts of interest exist in regard to this work.

REFERENCES

1. Albini A, Tosetti F, Li VW, et al. Cancer prevention by targeting angiogenesis. *Nat Rev Clin Oncol* 2012;9:498–509.
2. Cook KM, Figg WD. Angiogenesis inhibitors: current strategies and future prospects. *CA Cancer J Clin* 2010; 60:222–43.
3. Heath VL, Bicknell R. Anticancer strategies involving the vasculature. *Nat Rev Clin Oncol* 2009;6:395–404.
4. Chung AS, Wu X, Zhuang G, et al. An interleukin-17-mediated paracrine network promotes tumor resistance to anti-angiogenic therapy. *Nat Med* 2013;19:1114–23.
5. Seton-Rogers S. Tumour microenvironment: means of resistance. *Nat Rev Cancer* 2013; 13:607.
6. Chinot OL, Wick W, Mason W, et al. Bevacizumab plus radiotherapy-temozolomide for newly diagnosed glioblastoma. *New Engl J Med* 2014; 370:709–22.
7. Gilbert MR, Dignam JJ, Armstrong TS, et al. A randomized trial of bevacizumab for newly diagnosed glioblastoma. *New Engl J Med* 2014;370: 699–708.
8. Skyba DM, Price RJ, Linka AZ, et al. Direct in vivo visualization of intravascular destruction of microbubbles by ultrasound and its local effects on tissue. *Circulation* 1998;98:290–93.
9. Huang P, You X, Pan M, et al. A novel therapeutic strategy using ultrasound mediated microbubbles destruction to treat colon cancer in a mouse model. *Cancer Lett* 2013;335:183–90.

10. Liu Z, Gao S, Zhao Y, et al. Disruption of tumor neovasculature by microbubble enhanced ultrasound: a potential new physical therapy of anti-angiogenesis. *Ultrasound Med Biol* 2012;38:253–61.
11. Wood AK, Bunte RM, Cohen JD, et al. The antivascular action of physiotherapy ultrasound on a murine tumor: role of a microbubble contrast agent. *Ultrasound Med Biol* 2007;33:1901–10.
12. Hu X, Kheirolomoom A, Mahakian LM, et al. Insonation of targeted microbubbles produces regions of reduced blood flow within tumor vasculature. *Invest Radiol* 2012;47:398–405.
13. Wood AK, Bunte RM, Price HE, et al. The disruption of murine tumor neovasculature by low-intensity ultrasound-comparison between 1- and 3-MHz sonication frequencies. *Acad Radiol* 2008; 15:1133–41.
14. Bunte RM, Ansaloni S, Sehgal CM, et al. Histopathological observations of the antivascular effects of physiotherapy ultrasound on a murine neoplasm. *Ultrasound Med Biol* 2006;32:453–61.
15. Wood AK, Ansaloni S, Ziemer LS, et al. The antivascular action of physiotherapy ultrasound on murine tumors. *Ultrasound Med Biol* 2005;31:1403–10.
16. Gee MS, Saunders HM, Lee JC, et al. Doppler ultrasound imaging detects changes in tumor perfusion during antivascular therapy associated with vascular anatomic alterations. *Cancer Res* 2001; 61:2974–82.
17. Eichhorn ME, Klotz LV, Luedemann S, et al. Vascular targeting tumor therapy: non-invasive contrast enhanced ultrasound for quantitative assessment of tumor microcirculation. *Cancer Biol Ther* 2010;9:794–802.
18. Lin CY, Li JR, Tseng HC, et al. Enhancement of focused ultrasound with microbubbles on the treatments of anticancer nanodrug in mouse tumors. *Nanomedicine* 2012;8:900–7.
19. Zhong H, Li R, Hao YX, et al. Inhibition effects of high mechanical index ultrasound contrast on hepatic metastasis of cancer in a rat model. *Acad Radiol* 2010;17:1345–9.
20. Wu J, Nyborg WL. Ultrasound, cavitation bubbles and their interaction with cells. *Adv Drug Deliv Rev* 2008;60:1103–16.
21. Abbott JG. Rationale derivation of MI and TI—a review. *Ultrasound Med Biol* 1999;25:431–41.
22. Leite de Oliveira R, Deschoemaeker S, Henze AT, et al. Gene-targeting of phd2 improves tumor response to chemotherapy and prevents side-toxicity. *Cancer Cell* 2012;22:263–77.
23. Weidner N, Semple JP, Welch WR, et al. Tumor angiogenesis and metastasis–correlation in invasive breast carcinoma. *New Engl J Med* 1991;324: 1–8.
24. Jacquemier JD, Penault-Llorca FM, Bertucci F, et al. Angiogenesis as a prognostic marker in breast carcinoma with conventional adjuvant chemotherapy: a multiparametric and immunohistochemical analysis. *J Pathol* 1998;184:130–5.
25. Zeng Z, Shen L, Li X, et al. Disruption of histamine h2 receptor slows heart failure progression through reducing myocardial apoptosis and fibrosis. *Clin Sci* 2014;127:435–48.
26. Vyas AR, Hahm ER, Arlotti JA, et al. Chemoprevention of prostate cancer by d,l-sulforaphane is augmented by pharmacological inhibition of autophagy. *Cancer Res* 2013;73:5985–95.
27. Prentice P, Cuschieri A, Dholakia K, et al. Membrane disruption by optically controlled microbubble cavitation. *Nat Phys* 2005;1:107–10.
28. Wood AK, Schultz SM, Lee WM, et al. Antivascular ultrasound therapy extends survival of mice with implanted melanomas. *Ultrasound Med Biol* 2010;36:853–7.
29. Lin CY, Tseng HC, Shiu HR, et al. Ultrasound sonication with microbubbles disrupts blood vessels and enhances tumor treatments of anticancer nanodrug. *Int J Nanomed* 2012;7:2143–52.
30. Carmeliet P, Jain RK. Angiogenesis in cancer and other diseases. *Nature* 2000;407:249–57.
31. Ribatti D, Nico B, Crivellato E, et al. The structure of the vascular network of tumors. *Cancer Lett* 2007;248:18–23.
32. Carmeliet P, Jain RK. Principles and mechanisms of vessel normalization for cancer and other angiogenic diseases. *Nat Rev Drug Discov* 2011; 10:417–27.
33. Nagy JA, Chang SH, Shih SC, et al. Heterogeneity of the tumor vasculature. *Semin Thromb Hemost* 2010;36:321–31.
34. Tse D, Stan RV. Morphological heterogeneity of endothelium. *Semin Thromb Hemost* 2010;36: 236–45.
35. Li Q, Du J, Yu M, et al. Transmission electron microscopy of vx2 liver tumors after high-intensity focused ultrasound ablation enhanced with SonoVue. *Adv Ther* 2009;26:117–25.
36. Clement GT. Perspectives in clinical uses of high-intensity focused ultrasound. *Ultrasonics* 2004;42: 1087–93.
37. Kiessling F, Huppert J, Palmowski M. Functional and molecular ultrasound imaging: concepts and contrast agents. *Curr Med Chem* 2009;16: 627–42.